# A SPECTRAL LINE SURVEY OF THE ULTRACOMPACT H II REGION G34.3+0.15. II: 155.3–165.3 GHZ

HUN–DAE KIM[1] , SE–HYUNG CHO[1] , CHANG–WON LEE[1] , AND MICHAEL G. BURTON[2,3]

[1]Taeduk Radio Astronomy Observatory, Korea Astronomy Observatory, Whaam-dong, Yusong-gu, Taejon 305-348, Korea

[2]School of Physics, University of New South Wales, Sydney, NSW 2052

[3]School of Cosmic Physics, Dublin Institute for Advanced Studies, 5 Merrion Square, Dublin 2, Ireland

E-mail: hdkim@newt.phys.unsw.edu.au

## ABSTRACT

A molecular line survey towards the UC H II region G34.3+0.15 from 155.3 to 165.3 GHz has been conducted with the TRAO 14-m radio telescope. Combined with our previous observations from 84.7 to 115.6 GHz and 123.5 to 155.3 GHz (Paper I), the spectral coverage of this survey in G34.3+0.15 now runs from 85 to 165 GHz. From these latest observations, a total of 18 lines from 6 species were detected. These include four new lines corresponding to $\Delta J = 0, \Delta K = 1$ transitions of the $CH_3OH$ E–type species, and two new lines corresponding to transitions from $SO_2$ and $HC_3N$. These 6 new lines are $CH_3OH[1(1) - 1(0)E]$, $CH_3OH[2(1) - 2(0)E]$, $CH_3OH[3(1) - 3(0)E]$, $CH_3OH[4(1) - 4(0)E]$, $SO_2[14(1, 13) - 14(0, 14)]$ and $HC_3N[18 - 17]$. We applied a rotation diagram analysis to derive rotation temperatures and column densities from the methanol transitions detected, and combined with NRAO 12-m data from Slysh et al. 1999. Applying a two-component fit, we find a cold component with temperature $13 - 16$ K and column density $3.3 - 3.4 \times 10^{14}$ cm$^{-2}$, and a hot component with temperature $64 - 83$ K and column density $9.3 \times 10^{14} - 9.7 \times 10^{14}$ cm$^{-2}$. On the other hand, applying just a one-component fit yields temperatures in the $47-62$ K range and column densities from $7.5-1.1 \times 10^{15}$ cm$^{-2}$.

Key words : H II region—ISM: individual (G34.3+0.15)—ISM: molecules—ISM: abundances—stars: formation—radio lines: ISM

## I. INTRODUCTION

Following the line surveys conducted by Kim et al. (2000; Paper I), we have extended observations to the 155.3–165.3 GHz range towards G34.3+0.15. Since observations from 160–165 GHz have not been reported before, this survey may yield new information on the molecules present in the source. To date, several molecular line surveys have been reported for OMC–1 (eg Johansson et al. 1984; Jewell et al. 1989; Turner 1989; Blake et al. 1986, 1996; Ziurys & McGonagle 1993; Schilke et al. 1997), for Sgr B2 (Cummins, Linke & Thaddeus 1986; Turner 1989; Sutton et al. 1991) and for G34.3+0.15 (Macdonald et al. 1996; Thompson et al. 1999; Kim et al. 2000, Alvey 2001). However, none of these have covered the 155.3–165.3 GHz range completely before.

The observations closest in frequency were made by Ziurys & McGonagle (1993), from 150–160 GHz in Orion–KL. Thus, we anticipated finding new lines in the unexplored region, from 160–165 GHz. In addition, as indicated by the FCRAO observations of Ziurys & McGonagle, many transitions of methanol, from a wide range of excitation energy, were expected to be seen. Our latest observations also provided an opportunity to re-examine our earlier rotation diagram analysis for methanol (Paper I), which indicated there were two components in G34.3+0.15, a cold and a hot core component.

In the hot core, the high abundances found for complex molecules such as $CH_3OH$, $CH_3CN$, $NH_3$ and $H_2CS$ cannot be explained purely by gas phase reactions. Mantle evaporation from grain surfaces containing H- or N-bearing molecules, induced by radiation from an embedded protostar, provide a better explanation (eg Caselli, Hasegawa & Herbst 1993; Charnley, Tielens & Millar 1992) for their abundance. As the species evaporate, the chemical composition changes. Observations of the various kinds of molecules present, and their relative abundances, can be used to follow the progress of star formation in a cloud through its affect on the surrounding medium. Within the $\sim 1000$ year dynamical age of the hot molecular cores there is not sufficient time for significant chemical evolution to occur in the gas-phase chemistry, so the hot core abundances should reflect conditions at the time of switch-on of the central source. For instance, van Dishoeck & Blake (1998) have outlined a scenario where different species exist at varying distances from a central protostar. Ices such as $N_2$ and $O_2$ exist furthest out, in the coldest gas (T < 20 K). $CO_2$ ice, $CH_3OH$ ice and $H_2O$ ice are found progressively closer to the source, as the temperature rises and various chemical processing on the grain surfaces occurs. In the hot core a variety of complex organic molecules are found, evaporated off the grain surfaces. These then partake in a complex

chemistry for $\sim 10^5$ years in the core, as it evolves towards an UC H II region.

## II.  THE ULTRACOMPACT H II REGION G34.3+0.15

G34.3+0.15 has a cometary morphology (Reid & Ho 1985) and high electron density ($n_e > 10^6$ cm$^{-3}$). It is a well-studied, complex, UC H II region. It has been argued that the cometary morphology and limb brightening can be explained with a moving-star bow shock model (eg Van Buren at al. 1990; Mac Low et al. 1991). Alternatively, Garay, Rodriguez & van Gorkom (1986) have proposed a champagne-flow model for G34.3+0.15, where the ionized region forms at the edge of the cloud, producing a cometary morphology as it expands in a density gradient (Akeson & Carlstrom 1996).

Several comprehensive studies of G34.3+0.15 have been reported in the literature. These include molecular line observations (Forster et al. 1990; Martin-Pintado et al. 1983; Carral, Welsh & Wright 1987), mapping the J=1-0 and J=2-1 transitions of $^{13}$CO and CO, the J=1-0 and J=3-2 transitions of HCO$^+$ (Matthews et al. 1987), and in the J=1-0 transition of H$^{13}$CO$^+$, H$^{13}$CN, HC$^{15}$N and SO ($2_2 - 1_1$) (Carral & Welch 1992). NH$_3$ observations have been made in the (J,K)=(2,2) and (J,K)=(3,3) inversion transitions (Garay & Rodriguez 1990), in (J,K)=(3,3) (Andersson & Garay 1986), (J,K)=(1,1)...(7,7), (J,K)=(2,1)...(9,8) (Henkel, Wilson & Mauersberger 1987) and in (J,K)=(1,1), (J,K)=(2,1) (Heaton et al. 1985).

Molecular line surveys have been conducted from mm to sub-mm wavelengths (Macdonald et al. 1996; Hatchell et al. 1998; Thompson et al. 1999; Kim et al. 2000; Alvey 2001). A detailed time-dependent model calculation adopting three components, halo, compact core and ultracompact core, for the chemistry has been presented by Millar, Macdonald & Gibb (1997). Continuum observations at 2.7 mm have been undertaken (Watt & Mundy 1999). From mid-infrared observations, two of the radio components (A and C) are also seen in the IR, and two additional IR clumps (E and F) exist, south of clump C (Campbell et al. 2000). After Orion–KL and Sgr B2, G34.3+0.15 is certainly one of the most intensively studied star-forming regions at radio wavelengths.

Its distance has been estimated as 3.7 kpc (Downes et al. 1980). Velocities of $\sim 54.0$ km s$^{-1}$ from recombination line observations (Downes et al. 1980; Wink et al. 1983, Garay et al. 1986) have been measured in the cometary region and $\sim 59.0$ km s$^{-1}$ in the ambient molecular cloud (Heaton et al. 1985). A core-halo structure was seen in observations of the NH$_3$(1, 1) and (2,2) inversion transitions (Heaton et al. 1985). A warm ($\sim 60$ K), dense core ($6.0 \times 10^5$ cm$^{-3}$) was identified from the (J,K)=(3,3) inversion line transition of ammonia (Andersson & Garay 1986). In Table 1, physical parameters inferred from these ammonia observations are listed.

## III.  OBSERVATIONS

The observations of G34.3+0.15 were made over two weeks in 2000 January–February, using the Taeduk Radio Astronomy Observatory (TRAO) 14-m telescope in Korea. The position observed was $\alpha(1950) = 18^h 50^m 46^s.3$ and $\delta(1950) = 01°11'13''.0$. The beam size at 150 GHz is $40''$ and the forward spillover and scattering efficiency ($\eta_{\text{fss}}$) of the telescope is 0.54. We employed two 256-channel filter banks in serial mode, each with a resolution of 1 MHz, and used a dual-channel SIS mixer receiver in single-sideband mode (SSB). Thus the total bandwidth was 512 MHz. During the observations, the typical system temperature was approximately 500–800 K, and the RMS noise temperature $\sim 0.03$ K. To minimise line mis-identifications, some additional observations were also conducted with a high-resolution (250 kHz) spectrometer of selected lines. However, this data had greater noise and was not used in the subsequent analysis (although we note that such data was used in Paper 1). We report that the TRAO pointing is accurate to within $8''$. Pointing checks were made twice a day, at the beginning and in the middle of the observations. Calibration was performed by the standard chopper-wheel method, yielding line intensities in units of $T_A^*$ (Ulich & Haas 1976).

## IV.  SPECTRAL DISPLAY AND LINE IDENTIFICATION

Spectra taken at the same local frequency were averaged and then baseline subtracted using the SPA data reduction package. The spectra shown in Figure 1 have been combined from two adjacent spectra observed with different local oscillator frequencies, thereby covering about 1 GHz bandwidth.

To perform line identifications, we used the Lovas catalogue (Lovas 1992) and the JPL catalogue (Pickett et al. 1998). The central frequencies of each line stronger than $3\sigma$ have been determined from Gaussian fitting, after correcting for a Doppler shift of 58 km s$^{-1}$. From 6 known species, a total of 18 lines, including two blended lines which are marked as "bld" and 6 new lines which are indicated as "n", have been detected (Table 2). Most of the methanol lines had previously been detected by Ziurys & McGonagle (1993) in their Orion–KL observations. The 6 newly detected lines are 4 new methanol E–types, SO$_2$ $14(1,13) - 14(0,14)$ and HC$_3$N $18 - 17$.

## V.  INDIVIDUAL MOLECULES

### (a)  New Lines

Four new lines corresponding to $v_t = 0, \Delta J = 0, \Delta K = 1$ transitions of E–type CH$_3$OH, and two new lines corresponding to two transitions from SO$_2$ and HC$_3$N, have been detected. These 6 new lines

**Table 1.** Physical parameters of G34.3+0.15 derived from ammonia observations[a]

| Component | L (pc) | $T_{ex}$ (K) | $n_{H_2}$ (cm$^{-3}$) | Reference |
|---|---|---|---|---|
| Extended envelope | 3.7 | 9 | $5 \times 10^3$ | 1 |
| Molecular core | 1.7 | 18 | $4 \times 10^4$ | 1 |
| Warm compact core | 0.1 | 60 | $6 \times 10^5$ | 2 |
| Hot ultracompact core | 0.03 | 185 | $7 \times 10^7$ | 3 |

[a] As quoted by Garay & Rodriguez (1990).
References: (1) Heaton et al. 1985; (2) Andersson & Garay 1986; (3) Garay & Rodriguez 1990.

**Table 2.** Observed Molecular Parameters[a]

| $\nu(obs)$[b] (GHz) | $T_A^*$ (K) | $\Delta v$ (km s$^{-1}$) | Species | Transition | $\nu$(rest) (GHz) | $\int T_A^* dv$ (K km s$^{-1}$) | Notes |
|---|---|---|---|---|---|---|---|
| 155.3194 | 0.14 | 7.97 | CH$_3$OH | 10(0)-10(-1) E | 155.3209 | 1.20 | |
| 155.9956 | 0.18 | 11.93 | $^{13}$CH$_3$OH | 7(0)-7(-1) E | 155.9943 | 2.28 | bld |
| | | | CH$_3$OH | 9(0)-9(-1) E | 155.9975 | | |
| 156.1264 | 0.17 | 6.47 | CH$_3$OH | 6(2)-7(1) A+ | 156.1277 | 1.15 | |
| 156.4882 | 0.19 | 7.23 | CH$_3$OH | 8(0)-8(-1) E | 156.4890 | 1.47 | |
| 156.6023 | 0.32 | 6.41 | CH$_3$OH | 2(1)-3(0) A+ | 156.6024 | 2.18 | |
| 156.8280 | 0.13 | 9.55 | CH$_3$OH | 7(0)-7(-1) E | 156.8285 | 1.22 | |
| 157.0487 | 0.09 | 6.49 | CH$_3$OH | 6(0)-6(-1) E | 157.0486 | 0.61 | |
| 157.1789 | 0.21 | 4.86 | CH$_3$OH | 5(0)-5(-1) E | 157.1790 | 1.06 | |
| 157.2460 | 0.25 | 5.86 | CH$_3$OH | 4(0)-4(-1) E | 157.2461 | 1.58 | |
| 157.2726 | 0.38 | 12.50 | CH$_3$OH | 1(0)-1(-1) E | 157.2707 | 5.05 | bld |
| | | | CH$_3$OH | 3(0)-3(-1) E | 157.2725 | | |
| 158.1070 | 0.22 | 5.17 | OCS | 13-12 | 158.1074 | 1.27 | |
| 158.9716 | 0.33 | 6.32 | SO | 3(4)-2(3) | 158.9718 | 2.20 | |
| 163.6054 | 0.11 | 7.17 | SO$_2$ | 14(1,13)-14(0,14) | 163.6052 | 0.82 | n |
| 163.7532 | 0.22 | 5.68 | HC$_3$N | 18-17 | 163.7534 | 1.32 | n |
| 165.0500 | 0.27 | 5.23 | CH$_3$OH | 1(1)-1(0) E | 165.0502 | 1.53 | n |
| 165.0609 | 0.26 | 6.05 | CH$_3$OH | 2(1)-2(0) E | 165.0611 | 1.73 | n |
| 165.0989 | 0.25 | 5.70 | CH$_3$OH | 3(1)-3(0) E | 165.0993 | 1.51 | n |
| 165.1895 | 0.22 | 9.19 | CH$_3$OH | 4(1)-4(0) E | 165.1905 | 2.11 | n |

[a] Molecules and their transitions detected in the frequency range of 155.3–165.3 GHz. Blended lines are marked with a "bld" in the notes column. New lines detections are indicated with an "n".
[b] Observed frequencies after correcting the Doppler shift with the velocity of local standard of rest, 58 km s$^{-1}$. The full-width half-maximum (FWHM) and antenna temperature ($T_A^*$) of each line are derived from Gaussian fitting.
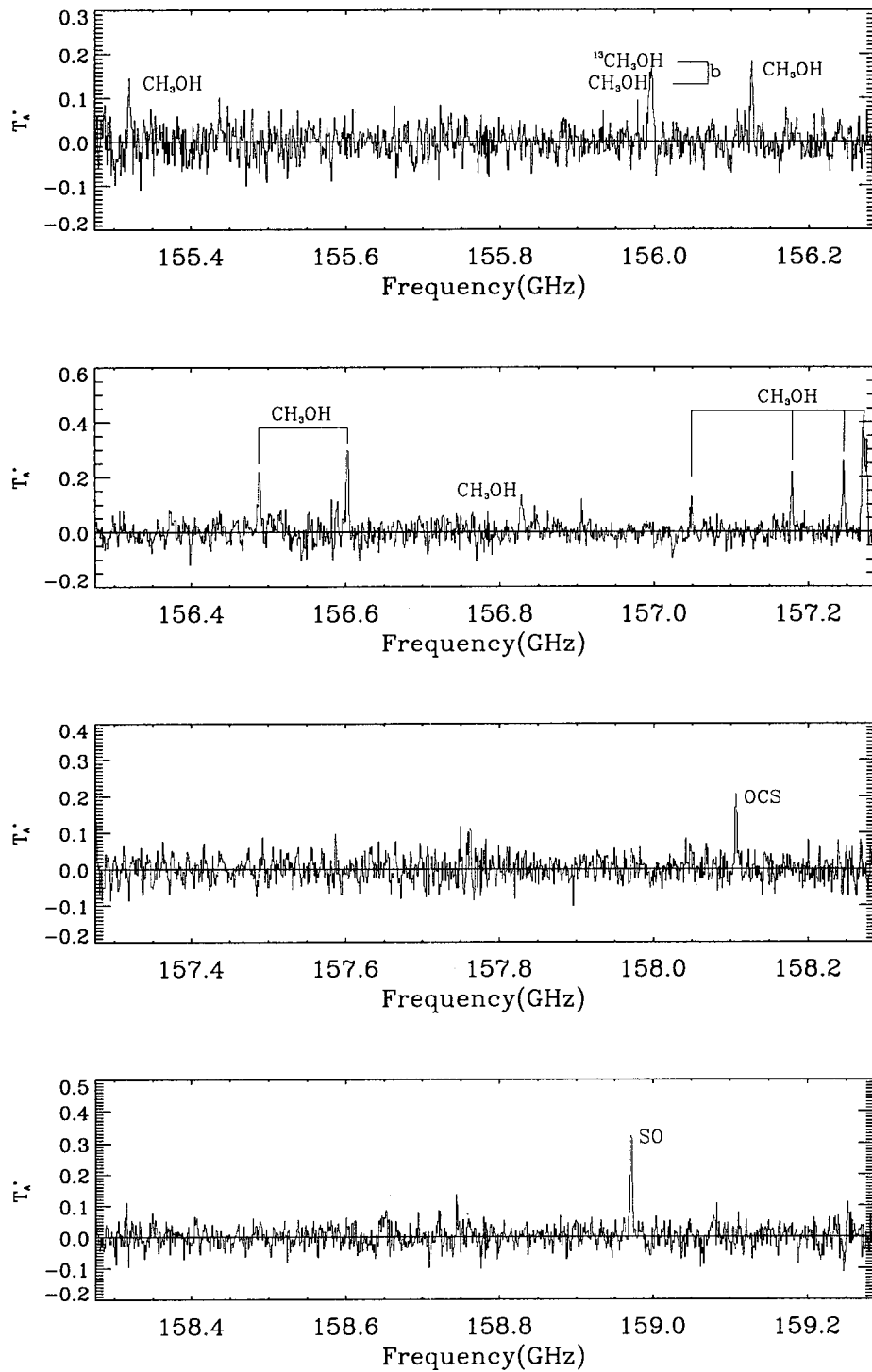
**Fig. 1.**— Spectra of G34.3+0.15, from 155.3 to 165.3 GHz, obtained during January-February, 2000 with the TRAO 14-m telescope. Each panel combines two neighbouring frequency measurements, to have about 1 GHz bandwidth.
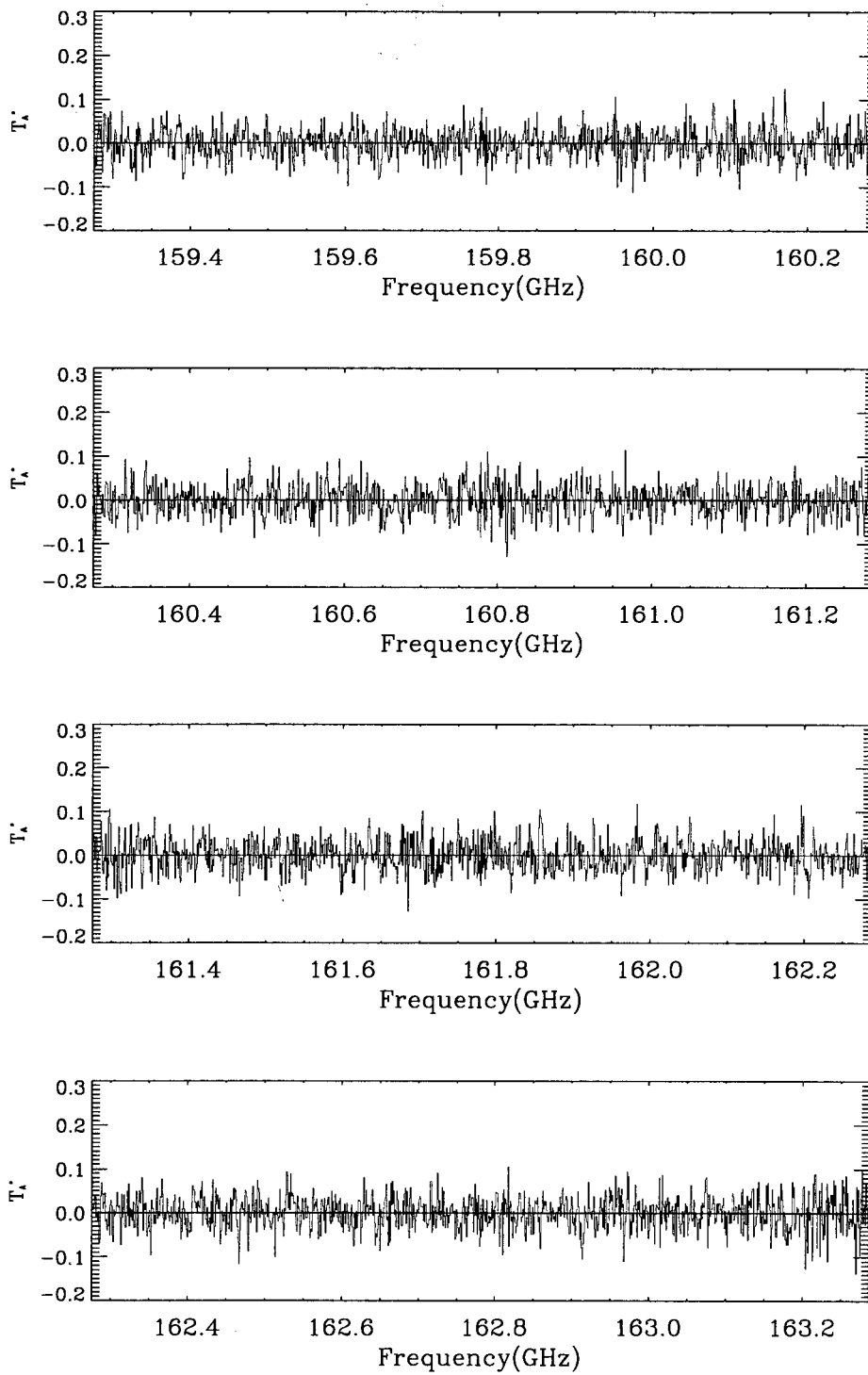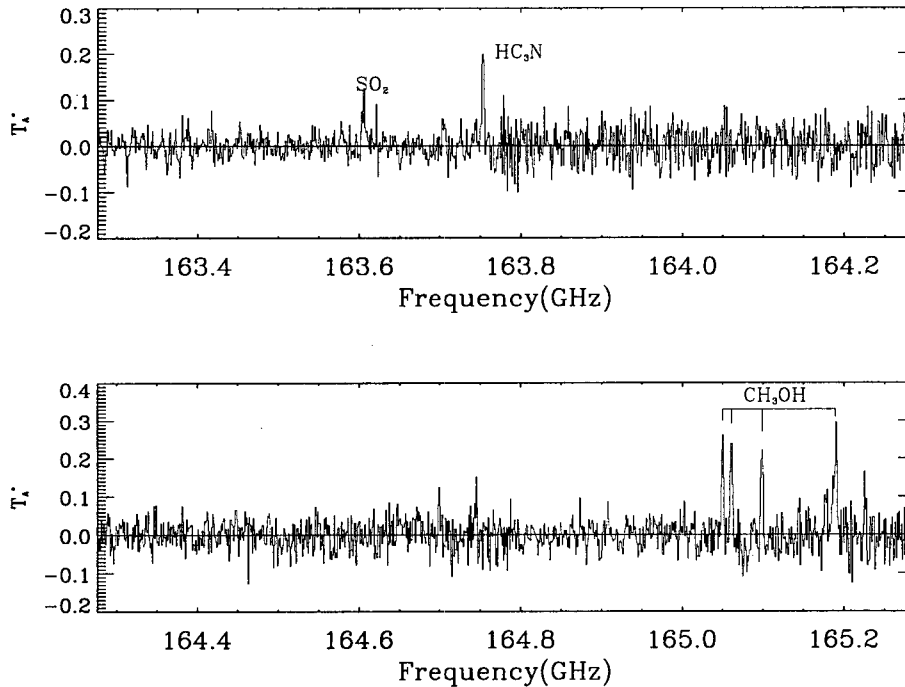
**Fig. 1.**— Continued

Fig. 1.— Continued

are identified as $CH_3OH[1(1) - 1(0)E]$, $CH_3OH[2(1) - 2(0)E]$, $CH_3OH[3(1) - 3(0)E]$, $CH_3OH[4(1) - 4(0)E]$, $SO_2[14(1,13)-14(0,14)]$ and $HC_3N[18-17]$ (see Figure 2). In addition, an unidentified line at 148.1119 GHz from Paper I we now identify as $CH_3OH$ 15[(0)-15(-1)] E, using the line list from Xu & Lovas (1997).

(b)   $CH_3OH$

A slightly asymmetric molecule, methanol ($CH_3OH$), is well-studied in the laboratory (eg Lees 1973; Herbst et al. 1984; Anderson, De Lucia & Herbst 1990). It has been widely used to study molecular clouds ever since the first detection by Ball et al. (1970) in Sgr B2 and Sgr A at 834 MHz, forming by transitions between the two levels of the lowest K-type doublet ($J_k = 1$). Subsequently, Barrett, Schwartz & Waters (1971) observed the K=2-1, J=4 to J=8 series of the E–type species at 25 GHz.

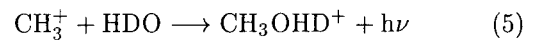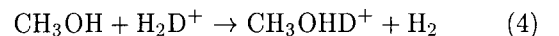$CH_3OH$ is thought to be produced in the gas phase reaction via the sequence of reactions (Smith & Adams 1977).

$$CH_3^+ + H_2O \longrightarrow CH_3OH_2^+ + h\nu \qquad (1)$$
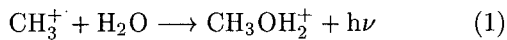
followed by dissociative association with an electron to give $CH_3OH$.

$$CH_3OH_2 + e^- \longrightarrow CH_3OH + H \qquad (2)$$

$$CH_3OH_2 + e^- \longrightarrow CH_3OH + \text{other products} \qquad (3)$$
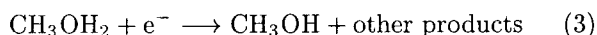
The transitions we detected between 155 and 160 GHz are similar to those seen by Ziurys & McGonagle (1993) in Orion–KL, except for our non-detection of the 157.5750 GHz line, and of a blended line at 157.2760 GHz. In the Orion-KL, the 157.5750 GHz line was detected with rather weaker antenna temperature (0.33 K) than the rest of methanol lines, which were observed with relatively strong emission ($\sim$ 2 K). We also did not detect any transitions from $^{13}CH_3OH$, unlike Ziurys & McGonagle. Macdonald et al. (1996) and Alvey (2001) also saw several $^{13}CH_3OH$ transitions in G34.3+0.15 from their 330–360 GHz and 210–264 GHz measurements.

It might have been expected that the deuterated $CH_3OD$ molecule would be detected. This is believed to be formed by simple proton exchange between $H_2D^+$ or $DCO^+$ and $CH_3OH$ or analogous manner with HDO substituted for $H_2O$ in equation 1 (Mauersberger et al. 1998; Anderson et al. 1988).

$$CH_3OH + H_2D^+ \rightarrow CH_3OHD^+ + H_2 \qquad (4)$$

$$CH_3^+ + HDO \longrightarrow CH_3OHD^+ + h\nu \qquad (5)$$

$$CH_3OH + DCO^+ \rightarrow CH_3OHD^+ + CO \qquad (6)$$

The deuterium enhancement is quite temperature dependent, increasing sharply at low temperature (Wootten, Loren & Snell 1982). However, it has become
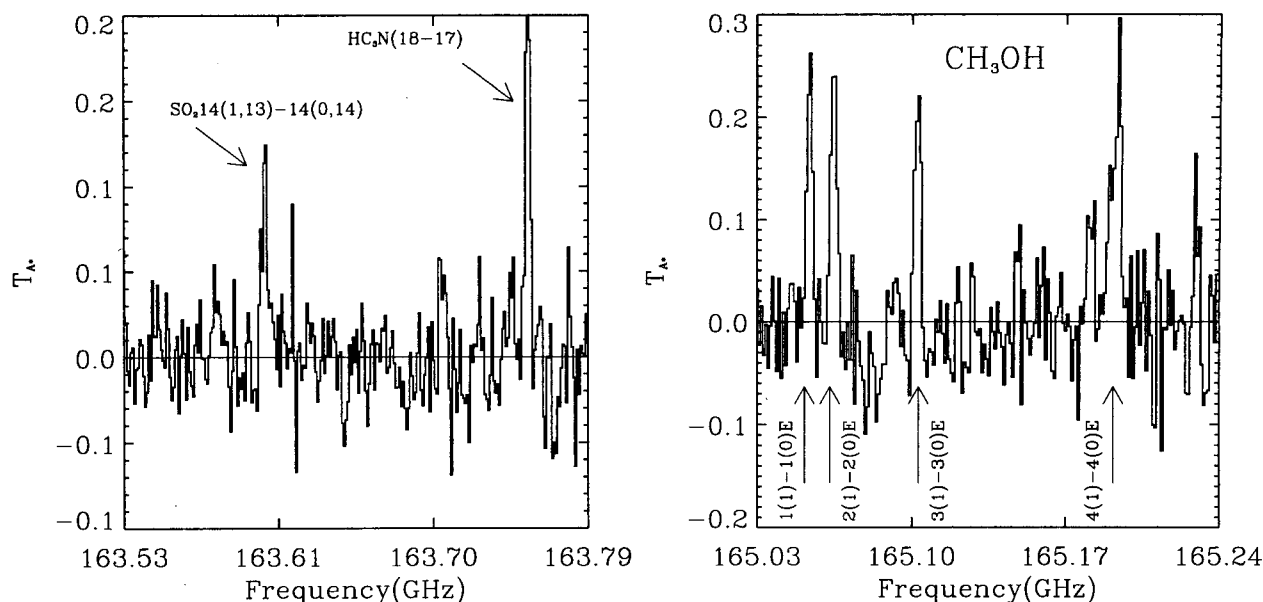
Fig. 2.— Spectra of the 6 new lines detected in G34.3+0.15, at 1 MHz resolution. The line identifications are: $SO_2[14(1,13) - 14(0,14)]$ and $HC_3N[18 - 17]$ (left), and $CH_3OH[1(1) - 1(0)E]$, $CH_3OH[2(1) - 2(0)E]$, $CH_3OH[3(1) - 3(0)E]$ and $CH_3OH[4(1) - 4(0)E]$ (right).

apparent that deuterium enhancement can be quite apparent that deuterium enhancement can be quite appreciable in hot core regions ($\sim$ 100 K) such as Orion–KL (Walmsley et al. 1987; Henkel et al. 1987). While several deuterated species, including $CH_3OD$, have clearly been measured in Orion–KL (Turner, 1989; Mauersberger et al. 1988; Jacq et al. 1993) and Sgr B2 (Gottlieb et al. 1979), no deuterated species were seen in our surveys of G34.5+0.15. A tentative detection of $CH_3OD$ at 143.742 GHz [5(1)-5(0) A-] was reported by Mauersberger et al. (1988), and DCN, DCCCN, HDO and $CH_3OD$ were all seen by Macdonald et al. (1996) and Alvey (2001) in G34.3+0.15. Since HDO was seen from G34.3+0.15, but the detection of $H_2D^+$ and $DCO^+$ from 85–360 GHz is negative, the production of $CH_3OD$ seems much alike to follow the reaction route of equation 5 than equation 4 or equation 6.

In view of these observational results, for the high degree of deuterium fractionation to be detectable, high kinematic temperature ($>$ 100 K), high abundance of D–bearing species, and high abundance of their pair molecules seem to be supplied.

### (c)   Lines not Seen in G34.3+0.15

Ziurys & McGonagle (1993) observed Orion–KL in the frequency range 150–160 GHz using the FCRAO 12-m telescope. This has a similar aperture to the TRAO telescope, with similar instrumentation and sensitivity. Table 3 lists lines seen in Orion–KL but not in G34.3+0.15. Almost all these lines are very weak, and so it was not surprising that they were not seen

in G34.3+0.15. However, the $SO_2$ [3(2,2)-3(1,3)] line seen at 158.20 GHz in Orion–KL is much stronger. It also arises from a low rotational level. Given our detections of higher excitation $SO_2$ 14[(1,13)-14(0,14)] (this paper) and $SO_2$ 5[(1,5)-4(0,4)] (Paper I) lines (both $\sim$ 0.1 K), the 158.20 GHz line might have been detectable. $CH_3CHO$, $HCOOCH_3$, $(CH_3)_2O$, $^{13}CH_3OH$ molecules have been seen in sub-mm observations of G34.3+0.15 (Macdonald et al. 1996). A line seen at 157.2760 GHz (Slysh et al. 1999) is evidently blended in our data.

Other heavy molecules seen in Orion–KL but not in G34.3+0.15, such as $CH_3CHO$, $HCOOCH_3$ and $(CH_3)_2O$, reflect that a greater dust mass and stronger radiation from the central sources may be supplied in order to be higher abundance of the species. Therefore, such saturated molecules are believed to trace relatively hotter regions of molecular clouds than simple linear molecules do.

Macdonald et al. (1996) found that the density of lines detected in G34.3+0.15 was 11.4 lines GHz$^{-1}$ to a detection limit in $T_A^*$ of about 0.5 K, which was similar to that in Orion–KL of 5.4 lines GHz$^{-1}$ at detection limit for $T_A^*$ of 1 K (Jewell et al. 1989), 8 lines GHz$^{-1}$ (Avery et al. 1992) to a detection limit of 0.1 K, and 9 lines GHz$^{-1}$ to a level of 0.8 K in $T_A^*$ (Greaves & White 1991). For the TRAO surveys from 85–155 GHz, 1.8 lines per GHz were found. The lower line density of lines per GHZ may reflect either beam dilution due to the small size of the hot core, and/or the sensitiv-

**Table 3.** Lines seen in Orion–KL but not in G34.3+0.15

| Frequency (GHz) | Molecule | Transition | $T_A^*$ (K) |
|---|---|---|---|
| 155.3421 | $CH_3CHO$ | 8(2,6)-7(2,5) A | 0.08 |
| 155.3897 | $SO_2$ | 20(6,14)-21(5,17) | 0.21 |
| 155.4045 | EtCN | 17(2,15)-16(2,14) | 0.20 |
| 155.4268 | EtCN | 18(1,18)-17(1,17) | 0.22 |
| 155.5068 | $^{34}SO$ | 3(4)-2(3) E | 0.37 |
| 155.5397 | $CH_3CHO$ | 8(4,4)-9(3,) A | 0.07 |
| 155.6958 | $^{13}CH_3OH$ | 8(0)-8(-1) E | 0.07 |
| 155.9943 | $^{13}CH_3OH$ | 7(0)-7(-1) E | 0.53 |
| 156.1652 | $HCOOCH_3$ | 22(3,19)-22(2,20) A | 0.07 |
| 156.1717 | EtCN | 18(0,18)-17(0,17) | 0.23 |
| 156.1866 | $^{13}CH_3OH$ | 6(0)-6(-1) E | 0.23 |
| 157.1354 | $SO_2$ | 33(4,30)-32(5,27) | 0.095 |
| 157.3442 | EtCN | 19(4,15)-19(3,16) | 0.04 |
| 157.5986 | $O^{13}CS$ | 13-12 | 0.07 |
| 157.9293 | $(CH_3)_2O$ | 13(3,11)-13(2,12)EA+AE | 0.23 |
| 157.9323 | | 13(3,11)-13(2,12)EE | |
| 157.9353 | | 13(3,11)-13(2,12)AA | |
| 157.9377 | $CH_3CHO$ | 8(1,7)-7(1,6) E | 0.08 |
| 157.9746 | $CH_3CHO$ | 8(1,7)-7(1,6) A | 0.06 |
| 158.1998 | $SO_2$ | 3(2,2)-3(1,3) | 0.71 |
| 158.2970 | $HCOOCH_3$ | 5(4,1)-4(3,2)A | 0.06 |
| 158.6920 | $H^{13}CCCN$ | 18-17 | 0.32 |
| 158.7043 | $HCOOCH_3$ | 13(3,11)-12(3,10)A | 0.30 |
| 158.5824 | $HCOOCH_3$ | 13(11,3)-12(11,2)A | 0.06 |
| | | 13(11,2)-12(11,1)A | |
| 159.6547 | $HCOOCH_3$ | 13(10,3)-12(10,2)E | 0.07 |
| 159.6631 | $HCOOCH_3$ | 13(10,3)-12(10,2)A | 0.12 |
| | | 13(10,4)-12(10,3)A | |
| 159.6712 | $HCOOCH_3$ | 13(10,4)-12(10,3)E | 0.13 |

Note. —Data from Ziurys & McGonagle (1993).

ity of system involving spectrometers employed. The resolution of spectrometer employed by Macdonald et al (1996) was 0.33 MHz, which is three times higher in resolution than TRAO observations from which two 1 MHz spectrometers were used in serial mode. On the other hand, the lower line density is also apparent in the hot core region of IRAS 17470–2853, as observed with the Mopra 22-m telescope in a limited band from 86–92 GHz (Kim, Ramesh & Burton 2001). In this source the lines detected were almost the same as those seen in G34.3+0.15 in the same band.

## VI. ROTATION DIAGRAM ANALYSIS FOR $CH_3OH$

Many methanol transitions have been detected in G34.3+0.15, both from the measurements we report here and our previous line surveys at 2 and 3 mm (Paper I). We adopt the rotation diagram method, described below, for their analysis.

Since methanol molecules of E and A–type have different internal characteristics, they should be dealt with separately. The standard radiative transfer equation can be simplified, if we assume that the lines are optically thin, and that the excitation temperature between the upper and lower transition is much higher than the cosmic background radiation temperature $(T_{BG})$:

$$\frac{N_u}{g_u} = \frac{3k \int T_R^* dv}{8\pi^3 \nu \mu^2 S g_I g_K} \tag{7}$$

$$\frac{N_u}{g_u} = \frac{N_T}{Q(T_{rot})} e^{-E_u/kT_{rot}} \tag{8}$$

$$N_T = \frac{3k \int T_R^* dv}{8\pi^3 \nu \mu^2 S g_I g_K} Q(T_{rot}) exp \left( \frac{E_u}{kT_{rot}} \right) \tag{9}$$

where $N_u$ is the upper state column density, $g_u$ is the upper state statistical weight, $T_{rot}$ is the rotational ex-

**Table 4.** CH$_3$OH Parameters Used for Rotation Diagram Analysis.

| Transition | Frequency (GHz) | $\int T_R^* dv$ (K km s$^{-1}$) | E$_u$/k (K) | $S\mu^2$ | Notes |
|---|---|---|---|---|---|
| 8(0)-7(1)A+ | 95.1694 | 2.70 | 83.6 | 7.210 | Paper I |
| 2(1)-1(1)A+ | 95.9143 | 2.55 | 21.5 | 1.178 | Paper I |
| 2(-1)-1(-1)E | 96.7394 | 7.34 | 11.6 | 1.176 | Paper I |
| 2(0)-1(0)A+ | 96.7414 | 9.37 | 7.0 | 1.567 | Paper I |
| 2(0)-1(0)E | 96.7446 | 2.49 | 19.2 | 1.567 | Paper I |
| 2(1)-1(1) E | 96.7555 | 0.84 | 27.1 | 1.207 | Paper I |
| 6(2)-7(1) A− | 132.6219 | 2.06 | 87.7 | 2.032 | Paper I |
| 6(-1)-5(0) E | 132.8908 | 8.41 | 53.4 | 3.683 | Paper I |
| 3(-1)-2(-1) E | 145.0975 | 2.94 | 18.6 | 2.350 | Paper I |
| 3(0)-2(0) A+ | 145.1032 | 3.59 | 13.9 | 2.351 | Paper I |
| 3(2)-2(2) E | 145.1264 | 0.43 | 38.9 | 1.308 | Paper I |
| 3(1)-2(1) E | 145.1319 | 0.65 | 34.1 | 2.415 | Paper I |
| 3(1)-2(1) A− | 146.3683 | 4.84 | 28.6 | 2.094 | Paper I |
| 9(0)-8(1) A+ | 146.6188 | 5.29 | 104.5 | 8.313 | Paper I |
| 11(0)-11(-1) E | 154.4258 | 2.15 | 165.2 | 7.652 | Paper I |
| 10(0)-10(-1)E | 155.3208 | 2.22 | 138.3 | 7.480 | |
| 6(2)-7(1) A+ | 156.1277 | 1.15 | 86.5 | 1.918 | |
| 8(0)-8(-1) E | 156.4890 | 3.18 | 95.7 | 6.792 | |
| 2(1)-3(0) A+ | 156.6024 | 4.03 | 20.2 | 1.996 | |
| 7(0)-7(-1) E | 156.8285 | 2.36 | 77.2 | 6.281 | |
| 6(0)-6(-1) E | 157.0486 | 1.15 | 60.9 | 5.667 | |
| 5(0)-5(-1) E | 157.1790 | 1.96 | 47.0 | 4.961 | |
| 4(0)-4(-1) E | 157.2461 | 2.92 | 35.4 | 4.173 | |
| 1(1)-1(0) E | 165.0502 | 2.83 | 22.4 | 1.346 | |
| 2(1)-2(0) E | 165.0611 | 3.10 | 27.1 | 2.236 | |
| 3(1)-3(0) E | 165.0993 | 2.80 | 34.1 | 3.116 | |
| 4(1)-4(0) E | 165.1905 | 3.91 | 43.3 | 3.980 | |

citation temperature, $k$ is Boltzmann's constant, $Q$ is the partition function, $g_I$ and $g_K$ are the nuclear and K–level degeneracies respectively, $E_u$ is the upper state energy, $\mu$ is the permanent dipole moment, $S$ is the line strength, and $N_T$ is the total column density. We introduce forward spillover and scattering efficiency, $\eta_{fss}$, to derive the line intensity, $\int T_R^* dv = \int T_A^* dv / \eta_{fss}$. A formal uncertainty $\Delta W = \int T_R^* dv$ may be calculated for each point solely from the rms channel-to-channel noise and is given by $\Delta W = m^{-1/2}\sigma$, where m is number of channels of the line. The typical $3\sigma$ of $\Delta W = 0.06 - 0.07$ K km s$^{-1}$, which is negligible compared with the dominant uncertainties such as calibration and pointing errors (Turner 1991). Therefore, error estimation related with $\Delta W$ is not performed in our rotation diagram analysis.

In the high temperature approximation, the total statistical weights of the methanol A and E species are expected to be equal, with the form of the partition function as follows (Turner 1991; Blake et al. 1987)

$$Q = Q(A + E) = 2[\pi(kT)^3/h^3ABC]^{1/2} \qquad (10)$$

The molecular parameters for methanol E–type transitions, such as line strength $(S)$, upper state energy $(E_u)$ and the rotational constants (A, B, C) have been taken from Anderson, De Lucia & Herbst (1990), and are summarized in Table 4. We take the rotational constants of the E and A species to be the same, though there are marginal differences in them. The electric dipole moment of a–type ($\Delta K$=0) is 0.899 Debye and 1.44 Debye for b–type transitions ($\Delta K$=1) (Sastry et al. 1981).

The upper state energy values are a little different from the methanol data (Lees 1973) we used in Paper I. Degeneracies, $g_i$ and $g_k$, for the E types are 1 and 2, and for A types are 2 and 1, respectively (Turner 1991). The rotation temperature $(T_{rot})$ can be derived by plotting $\ln[3kc\int T_R^*dv/8\pi^3\nu\mu^2Sg_Ig_K]$ versus $E_u/k$ and then performing a least squares straight line fit.

Initially, partition function values were derived by fitting the data, which are calculated assuming assumption of various temperature conditions (Poynter & Pickett 1984). The results are consistent with those from an approximate calculation (see Table 5). Therefore, we adopt the partition function values from the

Table 5. Partition Function Values

| Temperature(T) | Approximation(Q(T)) | Sum over States(Q(T))[a] | $\Delta$[b] |
|---|---|---|---|
| 13.3 | 59.8 | 62.7 | -2.9 |
| 26.9 | 171.9 | 189.2 | -17.3 |
| 47.2 | 399.9 | 425.6 | -25.7 |
| 63.7 | 626.8 | 641.4 | -14.6 |
| 71.8 | 749.7 | 745.9 | 3.8 |
| 117.7 | 1573.3 | 1630.7 | -57.4 |

[a] Partition function values obtained from the second degree polynomial fit to the data, which were derived from sum over states (Poynter & Pickett 1984).
[b] The difference between approximate calculations and sum over states.

approximate calculation in our rotation diagram analysis. The total column density $(N_T)$ was derived using Equation 4.

A distinction is apparent at a temperature of $\sim 50$ K in the level column density distribution (see Figure 3). Fitting all the level populations (E and A–types) above and below 50 K separately (Figure 3, top-left) yields a cold component with a rotation temperature of 13 K and column density $3.4 \times 10^{14}$ cm$^{-2}$, and a hot component with a temperature of 64 K and column density $9.7 \times 10^{14}$ cm$^{-2}$. On the other hand, performing a one-component fit to all the data gives a rotation temperature of 62 K and column density $7.5 \times 10^{14}$ cm$^{-2}$.

Plotting just the E–type lines, and applying the threshold at 50 K, gives a cold component with a rotation temperature of 13 K and column density $3.3 \times 10^{14}$ cm$^{-2}$, and a hot component with a temperature of 64 K and column density $9.3 \times 10^{14}$ cm$^{-2}$. This is very similar to the values found including both E and A–types.

One component fits, to just the E and A–type transitions, separately, result in a rotation temperature of 72 K and a column density $7.2 \times 10^{14}$ cm$^{-2}$ for E–type methanol, and a temperature of 47 K and a column density $1.1 \times 10^{15}$ cm$^{-2}$ for A–type methanol

On the other hand, Macdonald et al. (1996) derived column density $(1.8 \times 10^{16}$cm$^{-2})$ for CH$_3$OH A-type and column density $(1.9 \times 10^{16}$ cm$^{-2})$ for E-type, and Alvey obtained column density $(2.0 \times 10^{15}$ cm$^{-2})$ for E$_u <$ 45 K (halo) and $9.6 \times 10^{15}$ cm$^{-2}$ for E$_u >$ 45 K (hot core) of E-type methanol from the observations in the frequency range of 210-260 GHz. More detailed results found from Macdonald and Alvey are given in the Table 6.

As evident from Figure 3, lines from the lower energy levels provide a good straight line fit, whereas those from higher energy levels show considerable scatter in the fit. This may reflect the optical depth of higher upper state lines, where emission from the hot core would expected to be significant. One point, at $E_u/k = 60$ K, is plotted with an open rectangle in Figure 3, since significant calibration errors are suspected in the determination of the line intensity, in comparison with

the measurements of Slysh et al. 1999.

Slysh et al. (1999) measured several methanol lines with the NRAO 12-m telescope. All the lines, except for one at 132.6219 GHz, arise from levels less than 60 K above ground, so cover a smaller energy range than our data. Hence they are only sensitive to the cold component. We applied the rotation diagram analysis to their data, deriving temperature of 27 K and column density $4.9 \times 10^{14}$ cm$^{-2}$ (Figure 3). When we combine their E–type data with our own we obtain a temperature of 16 K and column density $3.4 \times 10^{14}$ cm$^{-2}$ for the cold component and a temperature of 83 K and column density $8.9 \times 10^{14}$ cm$^{-2}$ for the hot component (Figure 3, lower-panel).

An abundance ratio, CH$_3$OH A/CH$_3$OH E $\sim 1.2$, is found. This is the same as found in Orion–KL (Menton et al. 1988). As discussed in §(b), no D–bearing species are observed to our detection limit of 0.1 K. Hence we derive an upper limit to the column density of $9.7 \times 10^{12} - 5.8 \times 10^{13}$ cm$^{-2}$ for CH$_3$OD, using the abundance ratio of CH$_3$OH/CH$_3$OD=0.01-0.06 found in Orion-KL (Mauersberger et al. 1988).

## VII. SUMMARY

We have undertaken molecular line surveys in the frequency range 155.3–165.3 GHz in G34.3+0.15. As a result, 18 distinct lines from 6 molecules have been detected. Of these 18 lines, 6 lines identified as SO$_2$[14(1, 13) – 14(0, 14)], HC$_3$N[18 – 17], CH$_3$OH[1(1) – 1(0)E], CH$_3$OH[2(1)–2(0)E], CH$_3$OH[3(1)–3(0)E] and CH$_3$OH [4(1) – 4(0)E], were newly discovered (Table 2, Figure 3). Combining this data with our previous measurements (Paper I), it seems likely that the methanol in G34.3+0.15 arises from at least two components: a cold halo with temperature $13 - 16$ K and column density $3.3 \times 10^{14} - 3.4 \times 10^{14}$ cm$^{-2}$, and a hot core with temperature $64 - 89$ K, column density $9.3 \times 10^{14} - 9.7 \times 10^{14}$ cm$^{-2}$. On the other hand, applying just a one-component fit yields temperatures in the $47 - 62$ K range and column densities from $7.5 - 1.1 \times 10^{15}$ cm$^{-2}$.

Derived temperatures of cold halo and hot core are well-consistent with those of halo and core derived from ammonia observations (Table 1) and with the parame-
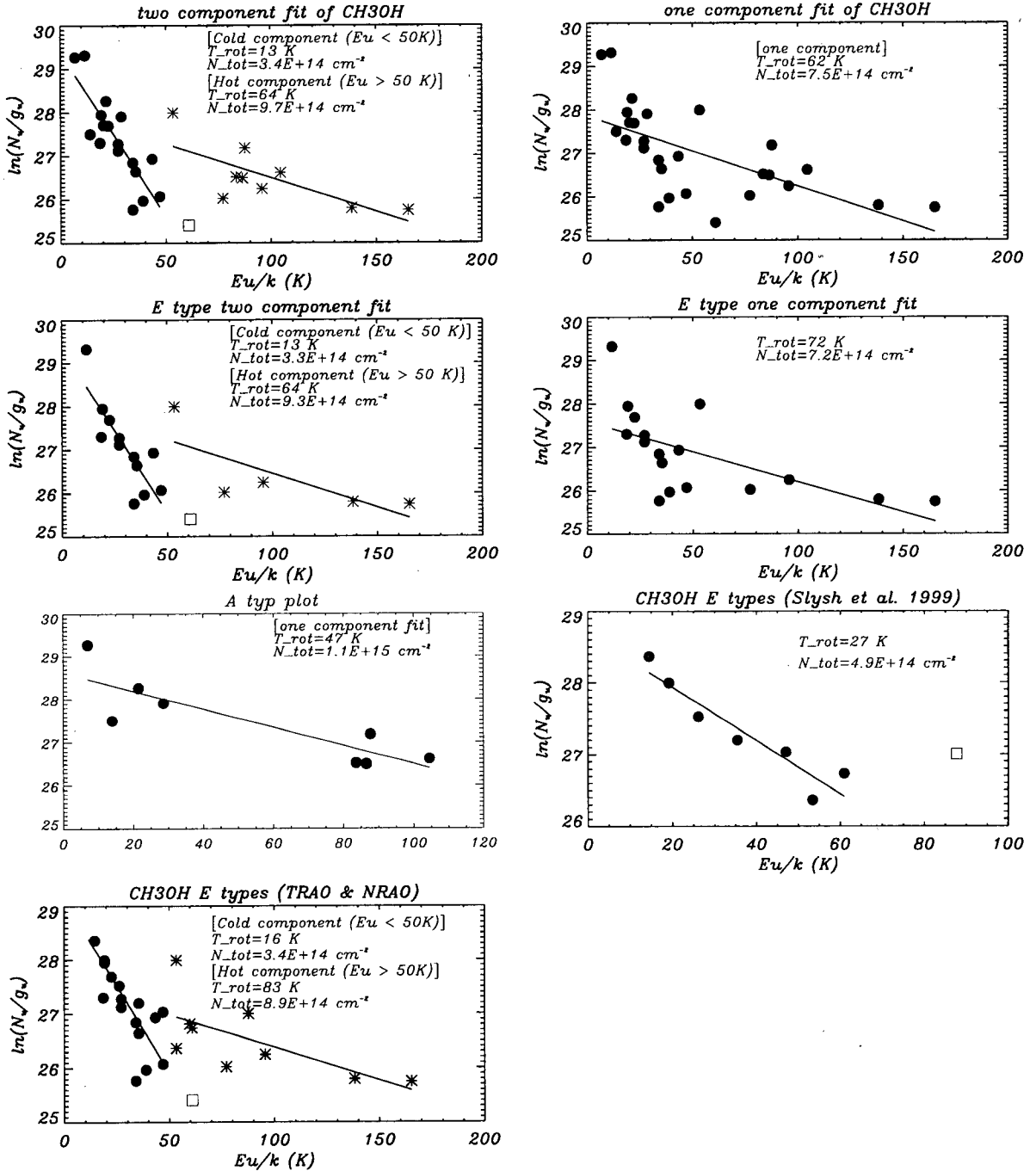
**Fig. 3.**— Rotation diagram analysis for the CH3OH data from G34.3+0.15 obtained with the TRAO telescope (this work and Paper I). Column densities, divided by level degeneracy (in $cm^{-2}$), are plotted against upper state energy level (in K). The top-left panel shows a two-component fit to all the E and A–type transitions (with the black circles showing those lines fit to first component, and the asterixes those to the second component), the top-right panel shows an one-component fit. The middle-left panel shows a two-component fit to the E–type lines only, and the middle-right panel shows an one-component fit to those lines. The lower-left panel shows an one-component fit to just the A–type transitions. The square, except for one point of lower-right panel, indicates a transition for which the flux calibration is in doubt. The lower-right panel for NRAO data only and the bottom panel combines the data with that from our TRAO survey and NRAO observations (Slysh 1999), and shows a two-component fit to all the E–type lines.

**Table 6.** Column Densities of $CH_3OH$

| Column density $(cm^{-2})$ | $T_{rot}$ (K) | Species | Envelope / Hot Core | Notes | Telescope |
|---|---|---|---|---|---|
| $3.4 \times 10^{14}$ | 13 | A & E types | Envelope | $E_u/k < 50\,K$ | TRAO 14-m |
| $9.7 \times 10^{14}$ | 64 | A & E types | Hot core | $E_u/k > 50\,K$ | TRAO 14-m |
| $7.5 \times 10^{14}$ | 62 | A & E types | | one component fit | TRAO 14-m |
| $3.3 \times 10^{14}$ | 13 | E types | Envelope | $E_u/k < 50\,K$ | TRAO 14-m |
| $9.3 \times 10^{14}$ | 64 | E types | Hot core | $E_u/k > 50\,K$ | TRAO 14-m |
| $7.2 \times 10^{14}$ | 72 | E types | | one component fit | TRAO 14-m |
| $1.1 \times 10^{15}$ | 47 | A types | | one component fit | |
| $4.9 \times 10^{14}$ | 27 | E types | | NRAO data (Slysh et al. 1999) | NRAO 12-m |
| $3.4 \times 10^{14}$ | 16 | E types | Envelope | TRAO & NRAO E–type data | TRAO & NRAO |
| $8.9 \times 10^{14}$ | 83 | E types | Hot core | TRAO & NRAO E–type data | TRAO & NRAO |
| $4.0 \times 10^{15}$ | 79 | A types | Envelope | $V_t = 0, E_u/k < 150\,K$ (Alvey 2001) | IRAM 30-m |
| $4.3 \times 10^{15}$ | 314 | A types | Core | $V_t = 0, E_u/k < 150\,K$ (Alvey 2001) | IRAM 30-m |
| $2.0 \times 10^{15}$ | 27 | E types | Envelope | $V_t = 0, E_u/k < 45\,K$ (Alvey 2001) | IRAM 30-m |
| $9.6 \times 10^{15}$ | 331 | E types | Core | $V_t = 0, E_u/k > 45\,K$ (Alvey 2001) | IRAM 30-m |
| $1.8 \times 10^{16}$ | $368 \pm 16$ | A-type | Core | Macdonald et al. (1996) | IRAM 30-m |
| $1.9 \times 10^{16}$ | $368 \pm 16$ | E-type | Core | Macdonald et al. (1996) | IRAM 30-m |

ters adopted in the chemical model (Millar, Macdonald, & Gibb (1997). Even so, column density, especially for hot core, derived from TRAO surveys are lower about one order than that derived from submillimeter observations, reflecting that beam dilution to the small size of hot core when we do observations with single dish telescope with high beam size seems to be significant as expected.

## REFERENCES

Akeson, R.L. & Carlstrom, J.E. 1996, ApJ, 470, 528

Alvey, N.D. 2001, PhD Dissertation, University of Kent

Anderson, T., Crownover, R.L., Herbst, E., & De Lucia, T. 1988, ApjS, 67, 135

Anderson, T., De Lucia, F.C. & Herbst, E. 1990, ApJS, 72, 797

Andersson, M. & Garay, G. 1986, A&A, 167, L1

Avery, L.W., Amano, T., Bell, M.B., et al., 1992, ApJ, 83, 363

Ball, J.A., Gottlieb, C.A., Lilley, A.E. & Radford, H.E. 1970, ApJ, 162, L203

Barrett, A.H., Schwartz, P.R. & Waters, J.W. ApJ, 168, L101

Blake, G.A., Sutton, E.C., Masson, C.R. & Phillips, T.G. 1986, ApJS, 60, 357

Blake, G.A., Sutton, E.C., Masson, C.R. & Phillips, T.G. 1987, ApJ, 315, 621

Brown, P.D., Charnley, S.B. & Millar, T.J. 1988, MNRAS, 231, 409

Campbell, M.F., Garland, C.A., Deutsch, L.K., Hora, J.L., Fazio, G.G., Dayal, A. & Hoffmann, W.F. 2000, ApJ, 536, 816

Carral, P. & Welch, W. 1992, ApJ, 385, 244

Carral, P., Welch, W. & Wright, M.C.H., 1997, RMxAA, 14, 506

Caselli, P., Hasegawa, T.I., Herbst, E. 1993, ApJ, 408, 548

Charnley, S.B., Tielens, A.G.G.M. & Millar, T.J. 1992, ApJ, 399, 71

Cummins, S.E., Linke, R.A. & Thaddeus, P. 1986, ApJ, 60, 819

Downes, D., Wilson, T.L., Bieging, J. & Wink, J. 1980, A&AS, 40, 379

Forster, J.R., Caswell, J.L., Okumura, S.K., Ishigueo, M. & Hasegawa, T. 1990, A&A, 231, 473

Garay, G. & Rodriguez, L.F. 1990, ApJ, 362, 191

Garay, G., Rodriguez, L.F. & van Gorkom, J.H. 1986, ApJ, 309, 553

Gottlieb, C.A., Ball, J.A., Gottlieb, E.W. & Dickinson, D.F. 1979, ApJ, 227, 422

Greaves, J.S. & White, G.J. 1991, A&AS, 91, 237

Hatchell, J., Thompson, M.A., Millar, T.J. & Macdonald, G.H. 1998, A&AS, 133, 29

Heaton, B.D., Matthews, N., Little, L.T. & Dent, W.R.F. 1985, MNRAS, 217, 485

Henkel, C., Wilson, T.L. & Mauersberger, R. 1987, A&A, 182, 137

Herbst, E., Messer, J.K., De Lucia, F.C. & Helminger, P. 1984, J. Molec. Spectrosc., 108, 42

Jacq, T., Walmsley, C.M., Mauersberger, R., Anderson, T., Herbst, E. & de Lucia, F.C. 1993, A&A, 271, 276

Jewell, P.R., Hollis, J.M., Lovas, F.J. & Snyder, L.E. 1989, ApJS, 70, 833

Johansson, L.E.B., et al. 1984, A&A, 130, 227

Kim, H.-D., Cho, S.-H., Chung, H.-S., Kim, H.-R., Roh, D.-G., Kim, H.-G., Minh, Y.-C. & Minh, Y.-K. 2000, ApJS, 131, 483 (Paper I)

Kim, H.-D., Ramesh, B. & Burton, M.G. 2001, PASA submitted

Kutner, M.L. & Ulich, B.L. 1981, ApJ, 250, 341

Lees, R.M. 1973, J. Phys. Chem. Ref. Data, 2, 205

Lovas, F.J. 1992, J. Phys. Chem. Ref. Data, 21, 181

Macdonald, G.H., Gibb, A.G., Habing, R., J. & Millar, T.J. 1996, A&AS, 119, 333

Mac Low, M.-M., Van Buren, D., Wood, D.O.S. & Churchwell, E. 1991, ApJ, 369, 395

Martin-Pintado, J., Wilson, T.L., Gardner, F.F. & Henkel, C. 1983, A&A, 117, 145

Matthews, N. et al. 1987, AA, 184, 284

Mauersberger, R., Henkel, C., Jacq, T. & Walmsley, C.M. 1988, A&A, 194, L1

Menten, K.M., Walmsley, C.W., Henkel, C. & Wilson, T.L. 1988, A&A, 198, 253

Millar, T.J., Macdonald, G.H. & Gibb, A.G. 1997, 325, 1163

Pickett, H.M., Poynter, R.L., Cohen, E.A., Delitsky, M.L., Pearson, J.C. & Muller, H.S.P. 1998, in "Submillimeter, Millimeter and Microwave Spectral Line Catalogue", J. Quant. Spectrosc. & Rad. Transfer, 60, 883

Poynter, R.L. & Pickett, H.M. 1984, in "Submillimeter, Millimeter, and Microwave Spectral Line Catalogue", JPL Publication 80-23 (2nd rev., Pasadena, California)

Reid, M.J. & Ho, P.T.P. 1985, ApJ, 288, L17

Sastry, K.V.L.N., Lees, R.M., Van Der Linde, J. 1981, J. Molec. Spectrosc., 88, 228

Schilke, P., Groesbeck, T.D., Blake, G.A. & Phillips, T.G. 1997, ApJS, 108, 301

Slysh, V.I., Kalenskii, S.V., Val'tts, I.E., Golubev, V.V. & Mead, K. 1999, ApJS, 123,515

Smith, D., and Adams, N. G. 1977, ApJ, 217, 741

Sutton, E.C., Jaminet, P.A., Danchi, W.C. & Blake, G.A. 1991, ApJS, 77, 255

Thompson, M.A., Macdonald, G.H. & Millar, T.J. 1999, A&A, 342, 809

Turner, B.E. 1989, ApJS, 70, 539

Turner, B.E. 1991, ApJS, 76, 617

Ulich, B.L. & Haas, R.W. 1976, ApJS, 30, 247

Van Buren, D., Mac Low, M.-M., Wood, D.O.S. & Churchwell, E. 1990, ApJ, 353, 570

van Dishoeck, E.F. & Blake, G.A. 1998, ARAA, 36, 317

Walmsley, C.M., Hermsen, W., Henkel, C., Mauersberger, R. & Wilson, T.L. 1987, A&A, 172, 311

Watt, A. & Mundy, L.G. 1999, 125, 143

Wink, J.E., Wilson, T.L. & Bieging, J.H. 1983, ApJS, 127, 211

Wootten, A., Loren, R.B. & Snell, R.L. 1982, ApJ, 255, 160

Xu, L.-H. & Lovas, F.J. 1997, J. Phys. Chem. Ref. Data, 26, 17

Ziurys, L.M. & McGonagle, D. 1993, ApJS, 89, 155